

LASER INTERFEROMETER GRAVITATIONAL WAVE OBSERVATORY
-LIGO-
CALIFORNIA INSTITUTE OF TECHNOLOGY
MASSACHUSETTS INSTITUTE OF TECHNOLOGY

Technical Note LIGO-T000077- 00- R 8/10/00

**TNI mode cleaner/
laser frequency stabilization
system**

Eric Black, Seiji Kawamura, Luca Matone, Shanti Rao

This is an internal working note
of the LIGO Project.

California Institute of Technology
LIGO Project - MS 51-33
Pasadena CA 91125
Phone (626) 395-2129
Fax (626) 304-9834
E-mail: info@ligo.caltech.edu

Massachusetts Institute of Technology
LIGO Project - MS 20B-145
Cambridge, MA 01239
Phone (617) 253-4824
Fax (617) 253-7014
E-mail: info@ligo.mit.edu

WWW: <http://www.ligo.caltech.edu/>

Contents

1	Introduction	2
2	Requirements	2
3	Topology	3
3.1	Experimental setup	3
3.2	The open loop transfer function	7
4	Effective frequency fluctuations	7
5	Measurements	8
5.1	Noise measurements	9
5.1.1	Shot noise and electronic noise	9
5.1.2	MC and laser noise	10
5.2	Spurious path measurement	10
5.3	Finesse measurement	11
5.4	Transfer function measurement	12
5.4.1	The coil driver transfer function measurement	12
5.4.2	First internal mass resonance	12
5.4.3	NPRO slow actuator	12
5.4.4	Old NPRO frequency stabilization servo	12
6	Further optimization	12
6.1	Modifications to the slow path	13
6.2	Modifications to the common path	13
A	The UGF measurement	14
B	The crossover frequency	14

Abstract

This document describes work done on the Thermal Noise Interferometer's mode cleaner/laser frequency stabilization servo while Seiji Kawamura was visiting, July 17 through August 11, 2000.

Keywords

Thermal Noise Interferometer

1 Introduction

This document describes the current frequency stabilization scheme developed for the Thermal Noise Interferometer (TNI). It consists of

1. an NPRO 126 laser 500mW and
2. a suspended triangular cavity, or mode-cleaner

designed to meet the requirement on the residual frequency fluctuation of

$$\delta\tilde{\nu} \leq 30 \text{ mHz}/\sqrt{\text{Hz}} \quad (1)$$

2 Requirements

The laser frequency noise is approximately

$$(2 \times 10^4/f) \text{ Hz}/\sqrt{\text{Hz}} \quad (2)$$

from 10 Hz to 10 kHz [1] If the desired displacement sensitivity for the test cavity is

$$\delta\tilde{x} = 10^{-19} \text{ m}/\sqrt{\text{Hz}} \quad (3)$$

then the tolerated residual noise is

$$\delta\tilde{\nu} = \frac{\nu_0}{L_0} \delta\tilde{x} = 3 \text{ mHz}/\sqrt{\text{Hz}} \quad (4)$$

where $\nu_0 = 3 \times 10^{14}$ Hz is the laser frequency and $L_0 = 1$ cm is the test cavity length. Assuming a conservative Common Mode Rejection Ratio (CMRR) of 10, the requirement can be relaxed to $30 \text{ mHz}/\sqrt{\text{Hz}}$.

In order to achieve such frequency stabilization, the design of the servo amplifier must have a gain G of approximately

$$\begin{aligned} G &= 7000 \text{ @ } 100 \text{ Hz} \\ G &= 700 \text{ @ } 1 \text{ kHz} \end{aligned} \quad (5)$$

2.

$$A = 100 \frac{V}{V} \quad (7)$$

is a common stage to the two paths. As of this writing, it is composed of an SR560 and a high-voltage (± 30 V) amplifier in series;

3.

$$E_{pzt} = \frac{\omega_1}{s + \omega_1} \frac{s + \omega_2}{\omega_2} \frac{V}{V} \quad (8)$$

describes the passive circuit, shown in fig.(3), build to compensate the high frequency path by acting on the PZT, where

$$\begin{aligned} \omega_1/2\pi &= 100\text{Hz} \\ \omega_2/2\pi &= 60\text{kHz} \end{aligned} \quad (9)$$

4.

$$E_{MC} = G_{MC} \frac{s + \omega_3}{\omega_3} \frac{\omega_4}{s + \omega_4} \frac{\omega_5}{s + \omega_5} \frac{V}{V} \quad (10)$$

describes the passive circuit, whose current configuration is shown in fig.(4) but will be replaced by the filter shown in fig.(9), that acts on the coil driver of the MC test mass, where

$$\begin{aligned} G_{MC} &= 2.5 \times 10^{-3} \\ \omega_3/2\pi &= 1\text{Hz} \\ \omega_4/2\pi &= 10\text{Hz} \\ \omega_5/2\pi &= 30\text{Hz} \end{aligned} \quad (11)$$

5. $P_{pzt} = 4\text{MHz/V}$ is the transfer function for the laser actuator and

$$P_{mc} = 13 \times \frac{\omega_p^2}{s^2 + \frac{\omega_p}{Q}s + \omega_p^2} \frac{\mu\text{m}}{V} \quad (12)$$

is the transfer function for the coil driver and suspension together, with a resonance at $\omega_p/2\pi = 1$ Hz and a damped quality factor Q of approximately 10;

6. $f_0 = 3 \times 10^{14}$ Hz and $L_0 = 0.5\text{m}$ are the nominal laser frequency and mode cleaner cavity length;

7. ν is the uncontrolled laser frequency fluctuations and

8. x_{mc} is the uncontrolled cavity length fluctuations.

Once in closed loop, the path of interest is the one to the laser and the block diagram can be greatly simplified as shown in fig.(2) where M [V/Hz] describes the IC, A and the MC path transfer functions.

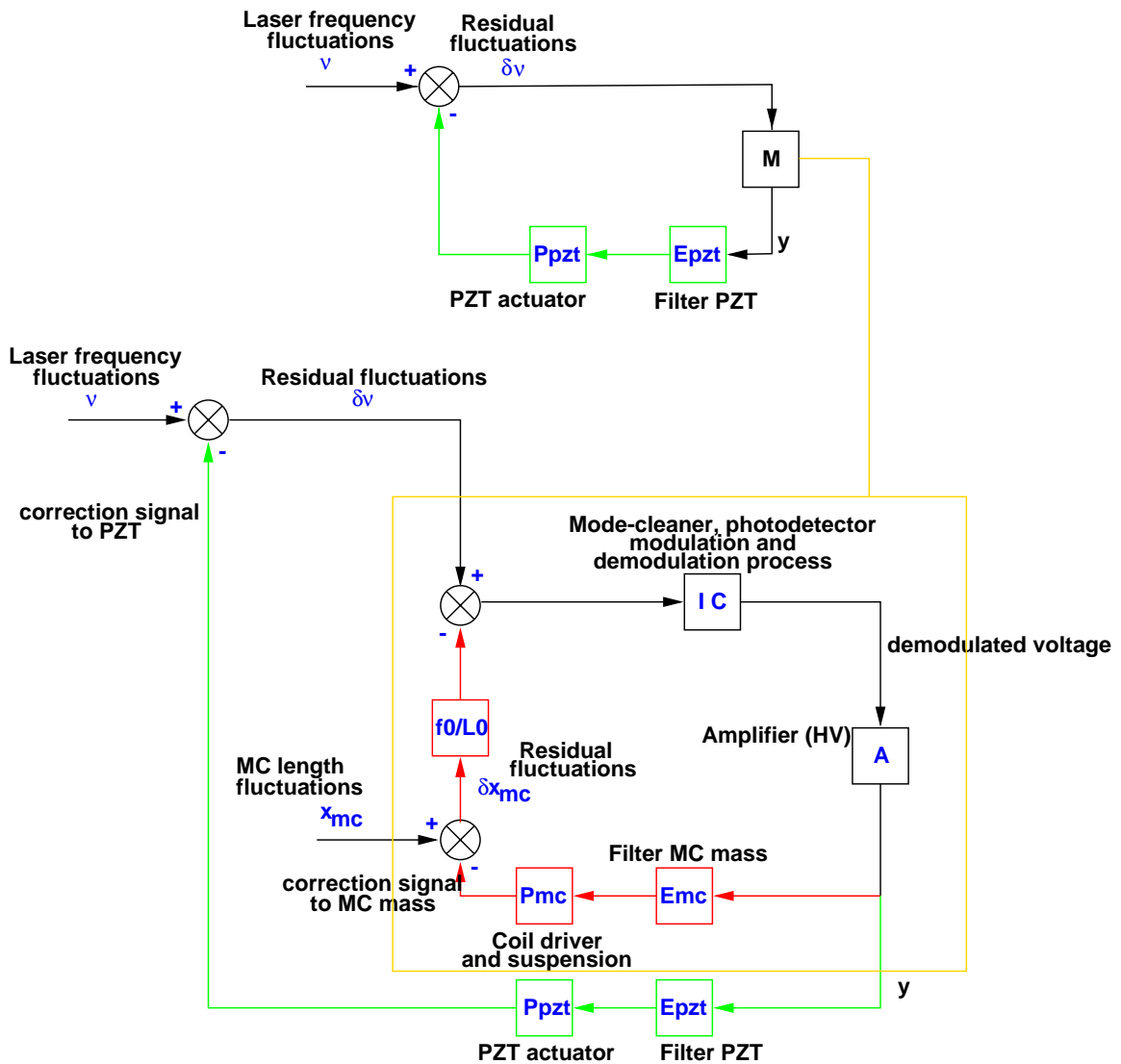


Figure 2: The block diagram of the experimental setup. The green path is acts on the laser PZT while the red path acts on the coil driver actuator of the MC end mass.

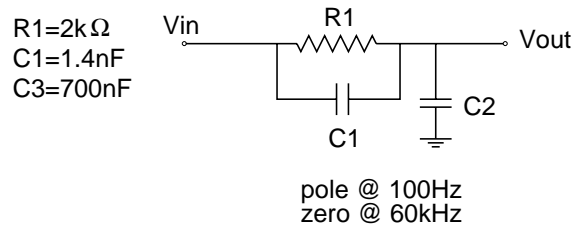
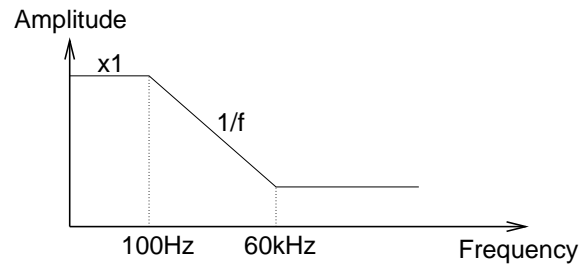


Figure 3:

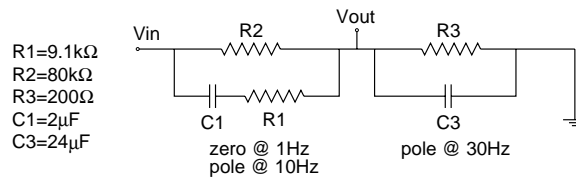
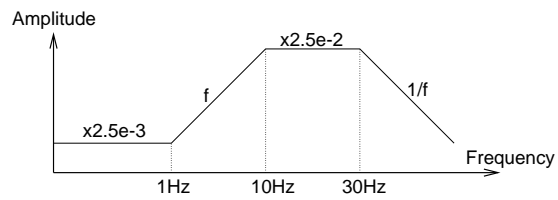


Figure 4:

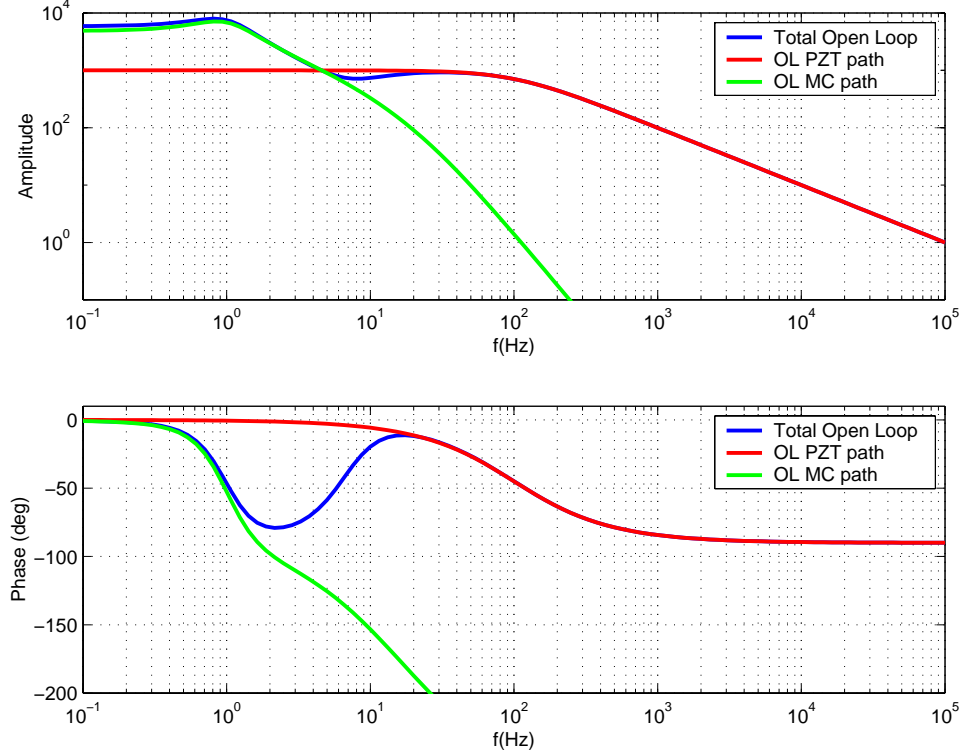


Figure 5: The open loop transfer function. Green: slow path; red: fast path; blue: global.

3.2 The open loop transfer function

A model of the open loop transfer function is shown in fig.(5), where the slow path is shown in green, the fast path is in red and the global transfer function is in blue. The model shows a DC gain of 5000 with a Unity Gain Frequency (UGF) of about 100 kHz and a crossover at about 4 Hz. We have measured the UGF and found it to be 80 kHz. We have ample phase margin (about 90°) at the UGF, and we expect to be able to push the UGF to 100 kHz without difficulty. We have measured the phase at UGF and found it to be 140° : the model does not take into account the PZT, amplifiers' and photodetector phase delays.

4 Effective frequency fluctuations

The laser frequency fluctuation is effectively attenuated only as we lock the laser onto the suspended mode cleaner cavity. However, no stabilization is achieved once we lock the laser onto the mode cleaner (the slow path) and therefore we'd like to investigate what is the effective frequency stabilization for the servo designed so far.

Referring to the top drawing in fig.(2), the residual frequency fluctuation $\delta\nu$ can be written as

$$\delta\nu = \frac{1}{1 + G_{\text{eff}}} \nu \quad (13)$$

where

$$G_{\text{eff}} = \frac{G_{\text{pzt}}}{1 + G_{\text{mc}}} \quad (14)$$

and

$$\begin{aligned} G_{\text{pzt}} &= IC \cdot A \cdot E_{\text{pzt}} \cdot P_{\text{pzt}} \\ G_{\text{mc}} &= IC \cdot A \cdot E_{\text{mc}} \cdot P_{\text{mc}} \cdot \frac{f_0}{L_0} \end{aligned} \quad (15)$$

Let's look at two different frequency regions: low frequency, where the mode cleaner follows the laser, and high frequency where the laser follows the mode cleaner.

1. For the low frequency region

$$G_{\text{mc}} > 1 \quad (16)$$

and the effective gain G_{eff} reduces to

$$G_{\text{eff}} \simeq \frac{G_{\text{pzt}}}{G_{\text{mc}}} \quad (17)$$

and the effective frequency stabilization is the ratio between the fast path gain G_{pzt} and the slow path gain G_{mc} ;

2. at high frequency

$$G_{\text{mc}} < 1 \quad (18)$$

and the effective frequency stabilization is then dominated by the fast path

$$G_{\text{eff}} \simeq G_{\text{pzt}} \quad (19)$$

5 Measurements

We performed a series of measurements to characterize the system:

1. noise, both electronic and photon-shot,
2. a spurious path around the PZT actuator,
3. the finesse of the mode cleaner,
4. the transfer functions of various stages in the loop, and
5. a possible test mass resonance measurement.

We will describe each of these measurements in more detail below.

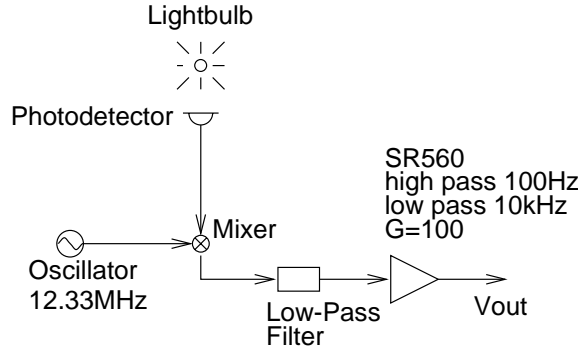


Figure 6:

5.1 Noise measurements

Three noise sources have been considered: electronic noise of demodulated signal, shot-noise and mode-cleaner/laser noise.

5.1.1 Shot noise and electronic noise

We measured the electronic noise of just the photodiode and demodulator and compared it with the shot noise of the system. We generated shot noise by shining a flashlight on the photodiode, producing the same dc power level as the laser. (Remember that the laser beam is heavily attenuated before it is sent into the photodiode.) The setup for this measurement is shown in fig.(6), where the output goes to a spectrum analyzer. We performed three kinds of measurements: the noise with the flashlight off, the noise with the flashlight on, and the noise with the SR560 disconnected from the photodiode and demodulator. In each case, the noise with the SR560 disconnected was substantially less than the noise with the photodiode and demodulator connected. We did this “zero” measurement both by grounding the SR560’s input and by disconnecting the photodiode and oscillator from the mixer, leaving the mixer and its low-pass filter connected to the amplifier. The noise was the same for both configurations and was typically more than 20 dB less than the noise with the electronics connected.

A variety of measurements of the electronic and shot noise were taken, with SR560 gains of 10^2 , 10^3 , and 10^4 . All measurements were done at 1 kHz. Shot noise and electronic noise combined was typically not more than 2 or 3 dB greater than electronic noise alone, indicating that the electronic noise and the shot noise are comparable. If N_{elec} is the electronic noise alone, and $N_{shot+elec}$ is the combined noise, we may find the shot noise by

$$N_{shot} = \sqrt{N_{shot+elec}^2 - N_{elec}^2}.$$

The electronic noise depends weakly on the gain of the SR560 and was found to be between 50 and $65 \text{ nV}/\sqrt{\text{Hz}}$ for all gains used. Not surprisingly, the shot noise did not depend on the SR560’s gain and was found to be $43.2 \pm 8.1 \text{ nV}/\sqrt{\text{Hz}}$. We may conclude that our measurement system is no more than about a factor of 2 noisier than the shot noise limit.

Furthermore, since $IC = 2.5 \mu\text{V}/\sqrt{\text{Hz}}$, the limit to frequency stabilization determined by shot

noise is

$$\frac{N_{\text{shot}}}{IC} = \frac{43\text{nV}/\sqrt{\text{Hz}}}{2.5\mu\text{V}/\sqrt{\text{Hz}}} = 1.7\text{m Hz}/\sqrt{\text{Hz}} \ll 30\text{m Hz}/\sqrt{\text{Hz}} \quad (20)$$

which is well below the required stability of $30 \text{ mHz}/\sqrt{\text{Hz}}$ without taking in consideration a CMRR of 10.

5.1.2 MC and laser noise

By locking the laser to the reference cavity and the mode cleaner to the laser, a low frequency measurement was possible of the noise level of both the mode cleaner and the laser. For the laser PZT V_{pzt} and coil driver V_{mc} monitors, we found that

$$\begin{aligned} V_{\text{pzt}} &= -40 \text{ dB } V_{\text{RMS}} @ 100\text{mHz} \\ V_{\text{mc}} &= -85 \text{ dB } V_{\text{RMS}} @ 100\text{mHz} \end{aligned} \quad (21)$$

corresponding to 40 kHz RMS for the laser and 400 kHz RMS for the mode cleaner: the mode cleaner is 10 times noisier than the laser @ 100 mHz. For this reason, a slow path is used to control the mode cleaner to the laser for frequencies below 100 mHz.

5.2 Spurious path measurement

The possible presence of spurious paths can limit the gain used in the servo system. For the TNI successful operation, it is mandatory to measure and resolve any possible spurious paths. One of them is the amplitude modulation generated when acting on the laser PZT and it can be described by the block diagram shown in fig.(7). Here, I describes the cavity transfer function, E the electronics,

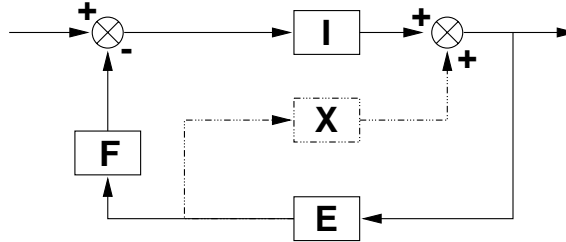


Figure 7:

F the PZT actuator and by X we indicate an unknown transfer function that describes the spurious link. The objective of this measurement is to quantify X and understand if it does indeed play a role.

The open loop transfer function G for the block diagram shown in figure is

$$G = IF \frac{E}{1 + XE} \quad (22)$$

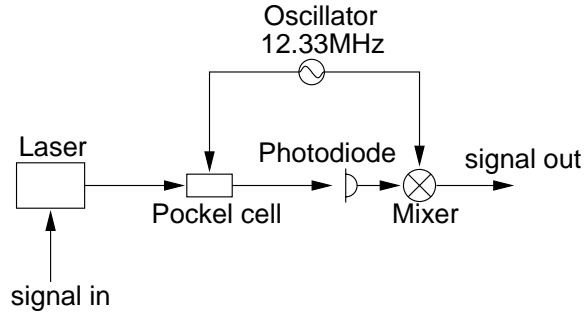


Figure 8:

If $X \cdot E > 1$ then

$$G \simeq \frac{I \cdot F}{X} \quad (23)$$

and the gain G is limited by the X transfer function.

From both the measurement of the open loop transfer function and the model shown in fig.(5), we induce that

$$IF = 10 \quad (24)$$

and we know that $E = 10$ @ 1 kHz.

Fig.(8) shows the experimental setup to measure the X transfer function. Laser light is again modulated and directed immediately toward the detection photodiode. A signal is sent to the PZT actuator and the output signal is the demodulated signal. A measurement of the ratio of the two signal, performed at 1kHz, has given

$$X \simeq 3 \times 10^{-5} \quad (25)$$

According to eq.(23), the limit in gain is

$$G < \frac{IF}{X} = \frac{10}{3 \times 10^{-5}} = 3 \times 10^5 \quad (26)$$

which is a limit high enough compared to the required gain.

5.3 Finesse measurement

The finesse has been measured in 3 different ways, always in closed loop and always measuring the cavity pole in the open loop transfer function.

The first measurement consisted in exciting the PZT actuator and recording the transfer function. This measurement dated back to the beginning of June 2000. The result has given a pole at 30 kHz, corresponding to a finesse of 5000. A drawback in the use of the PZT is an apparent phase delay at frequencies above 10 kHz.

Two other measurements were made in the month of July 2000. The first of the series was done by acting on the Pockels cell, therefore eliminating the PZT phase delay. This resulted in a cavity pole of 60 kHz corresponding to a finesse of 2500.

On the other hand, by locking on the first higher order mode, TEM 01, and repeating the measurement using again the Pockels cell, a cavity pole was found at 18 kHz, corresponding to a finesse of 8000. The cavity may have been contaminated.

For the frequency control, the electronics have been designed and created assuming a cavity pole @ 60 kHz.

5.4 Transfer function measurement

A series of transfer function measurements have been performed in open and closed loop. Here we briefly describe the most important measurements done so far.

5.4.1 The coil driver transfer function measurement

We also measured the coil driver efficiency by locking the mode cleaner to the laser with a UGF at 2 kHz. By injecting a sinusoid @ 100 Hz into the PZT actuator, and by monitoring the signal applied to the coil driver, we inferred an efficiency of 13 $\mu\text{m}/\text{V}$ at dc assuming a pendulum resonance at 1 Hz.

5.4.2 First internal mass resonance

While locking the mode cleaner to the laser, with a UGF at 500 Hz, we observed a resonance at 27.9 kHz, which we suspect may be an internal mode of the mode cleaner mirrors. The system was able to acquire and hold lock despite this resonance.

5.4.3 NPRO slow actuator

We were able to measure the temperature actuator (slow) of the laser in use. The amplitude of the transfer function rolled off as f^{-2} above 0.2 Hz, but its phase did not hold steady at 180°, as one would expect from Bode's gain-phase relations. This actuator may exhibit some nonlinear behavior above 0.2 Hz.

5.4.4 Old NPRO frequency stabilization servo

Transfer functions from INTI/PC OUT INTI/FAST OUT and gain settings have been measured and studied, but we are not using that unit in our present configuration.

6 Further optimization

One last optimization was performed on the electronics. While the electronics described thus far has been built, tested and in use, the last optimization was only tested with the aid of the low-noise SR560 preamplifiers and temporary electronics. At the writing of this document, a board is being built with

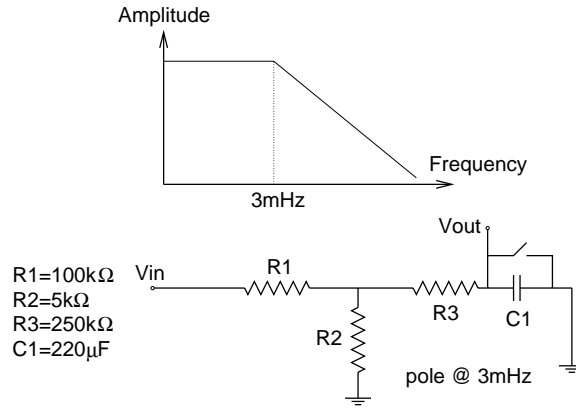


Figure 9:

the new features. These new features would improve the effective frequency stability of the laser beam.

6.1 Modifications to the slow path

In order to improve the current apparatus, the idea is to limit the slow path bandwidth to 3 mHz. As a consequence, higher gain is necessary but we are limited by the HV power supply of ± 30 V. By replacing the HV power supply with one delivering ± 50 V (since the pzt path can only accept up to ± 50 V), we can obtain the necessary gain to keep the mode cleaner locked to the frequency excursions. The passive filter replacing the slow path electronics is shown in fig.(9) (recall that the filter used previously is shown in fig.(4)). The switch shown in figure enables or disables the filter due to the high capacitance.

6.2 Modifications to the common path

We are also planning, but not yet tested, the use of the *boosts* located at 10 kHz. Both boosts would integrate up to 10 kHz and then become flat. We can afford to have two boosts due to a fairly large phase margin.

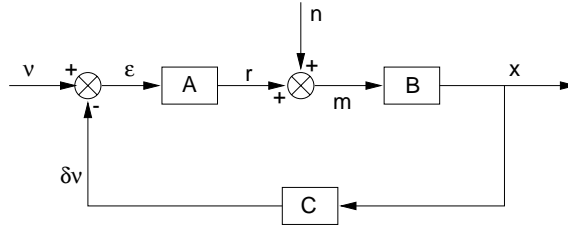


Figure 10:

Appendix

In this appendix we describe clever methods to measure directly the UGF point and crossover frequencies of the servo's open loop transfer function.

A The UGF measurement

It is possible to measure the OL transfer function of a servo system, in closed loop, without measuring the CL transfer function first. This is shown in fig.(10) where ν is the free laser frequency fluctuations and ABC is the OL transfer function. By injecting a signal n anywhere in the chain, and reading the signals right before and after the injection point (in this case signal r and signal m), then it can be shown with some algebraic manipulation that

$$\begin{aligned} \frac{r}{n} &= -\frac{ABC}{1+ABC} \\ \frac{m}{n} &= \frac{1}{1+ABC} \\ \frac{r}{m} &= -ABC \end{aligned} \tag{27}$$

B The crossover frequency

The crossover frequency can be found by measuring at what frequency

$$\frac{G_{pzt}}{G_{mc}} = 1 \tag{28}$$

References

- [1] Rich Abbott, James Mason, and Rick Savage *NPRO frequency stabilization LIGO-T970051-00-R (2-6-97)*.